### METALLURGICAL CONTROL OF

# **FATIGUE CRACK PROPAGATION IN ALLOY 718**

Keh-Minn Chang

GE Corporate Research and Development P.O. Box 8 Schenectady, NY 12301

# **Abstract**

Fatigue crack growth behavior in high-strength superalloys has been categorized into two domains: cycle-dependent and time-dependent. Alloy 718, which was strengthened by a low volume fraction of precipitate phases, began to show time-dependent fatigue crack propagation at temperatures above 500 °C. In the time-dependent domain, the crack growth resistance of alloy 718 could be improved by the addition of Cr content, or by the deformed grain structure produced through thermomechanical processing. Grain size was found to be the only factor affecting the cycle-dependent crack growth rate, but the effect is not significant.

### Introduction

Because of its unique characteristics, alloy 718 has been the most popular superalloy for gas turbine engine applications. The alloy offers good castability, workability, and weldability so that the processing cost becomes minimum. Turbine disks are one of the major applications for alloy 718. Conventionally, the tensile strength of available materials of construction limits the maximum stress level in turbine disk designs. Therefore, thermomechanical processing (TMP) was extensively used to improve alloy strength by controlling the grain size of the recrystallized microstructure [1,2].

When the maximum stresses are raised to a certain level, another phenomenon has become limiting, namely crack initiation and propagation in low cycle fatigue (LCF). Fatigue cracks grow under low cycle fatigue conditions if the cyclic stress intensity,  $\Delta K_{th}$ . In many cases, the higher the strength of a superalloy, the lower the threshold stress intensity. Consequently, the useful life of the component is dependent on the rate at which the fatigue crack will propagate through the alloy. Formal analysis of this life is the basis for the US Air Force design approach, Engine Structural Integrity Program (ENSIP) [3].

A comprehensive study on fatigue crack propagation (FCP) at engine service temperatures has been performed in alloy 718 [4]. In this paper the different crack growth behavior in high-strength superalloys, i.e., cycle-dependent and time-dependent FCPs, and the cause for the transition were identified experimentally. Two important metallurgical factors have been discovered to improve the crack growth resistance of this low precipitate content type of superalloys.

### **Experimental**

#### Material

A commercial premium grade alloy 718 forging of aircraft engine quality was obtained from the Wyman-Gorden Company, North Grafton, MA. The nominal composition of alloy 718 is Ni-19Cr-18.5Fe-3Mo-5.1Nb-0.9Ti-0.5Al-0.04C. A specific TMP schedule was applied to the disk forging in order to achieve a fine grain structure [5]. Direct aging treatments without a solution annealing were used to maintain the fine grain structure and to achieve a high tensile strength.

Specimen blanks were cut by wire-EDM from the disk forging, and their locations were identified. Some specimens received a standard heat treatment:  $1025 \,^{\circ}\text{C}/1 \,\text{h} + 720 \,^{\circ}\text{C}/8 \,\text{h} + 620 \,^{\circ}\text{C}/10 \,\text{h}$ . The one-hour solution treatment at  $1025 \,^{\circ}\text{C}$  dissolved all intermetallic precipitates except isolated MC carbide particles. Recrystallization and grain growth occurred during solutioning to develop an equiaxed grain structure of ASTM 7 (35  $\mu$ m).

Several laboratory heats were prepared by vacuum induction melting (VIM) and cast into chilled, cylindrical copper molds. Each ingot was homogenized at 1200 °C for 24 h, and then forged into plates according to the conventional wrought superalloy practice. One series of plate forgings with a nominal composition of alloy 718 was used to study the TMP effect. Another series was designed to vary the Cr content in alloy 718 with a minimum change in alloy strength.

## **Mechanical Testing**

Fatigue crack growth rate, da/dN, was measured by employing single-edge-notched (SEN) plate type specimens. The detailed experimental setup and testing procedure have been reported elsewhere [6]. Crack length was monitored continuously by using a reversing dc potential drop technique. An Instron servohydraulic system was equipped with a three-zone resistant furnace to provide a uniform temperature in the specimen with minimum electric noise. The system was also equipped with a custom-designed

microprocessor for data acquisition and machine control. To examine the environmental effect, some specimens were tested in a high temperature vacuum chamber. The vacuum system used a mechanical pump and a cryopump to keep a high vacuum better than 10<sup>-6</sup> torr throughout the test. The crack length was monitored by the same dc potential drop method as that used in air.

To evaluate the effect of a selected metallurgical factor on FCP, the crack growth rate was measured at temperatures from 400 to 650 °C with three different fatigue waveforms. A sinusoidal fatigue cycle of 0.33 Hz (designated as 3-s waveform) has been adopted as the standard in the aircraft engine industry. A 60X slower fatigue cycle of 0.0055 Hz (designated as 180-s waveform) allows verification of frequency effects on FCP. To better simulate the real service condition of a turbine engine component, a third fatigue waveform consisting of a 0.33 Hz sinusoidal fatigue cycle and a 177-s hold time at the maximum load of each cycle was used (designated as 3+177-s waveform). The latter two fatigue waveforms have the same cycle period, 180 s.

Tensile tests were performed in a high-temperature Instron machine; the yield strength was determined by the 0.2% offset technique as described by ASTM E8 standard procedure. Subsized round tensile specimens with shouldered ends were employed. The initial strain rate was 0.5 /min.

# Microscopy

Metallography of each specimen was performed according to standard laboratory procedures. Grain size was revealed by an etchant of 40 ml HCl + 10 ml HNO<sub>3</sub> + 30 ml H<sub>2</sub>O<sub>2</sub>. Fractography of each fatigue specimen was performed in a scanning electron microscope (SEM) to determine the cracking fracture mode under different fatigue waveforms.

#### Results and Discussion

### Crack Growth Behavior

The as-received disk forging had a fine grain structure as expected. Figure 1 shows the typical metallography obtained from the center of the forging. Equiaxed grains resulting from the TMP process have a grain size of ASTM 11 (5-10  $\mu$ m). The stringers, most of them  $\delta$ -Ni<sub>3</sub>Nb precipitates, aligned along the flow line of the forging. These precipitates existed at forging temperatures and prevented the grain growth.

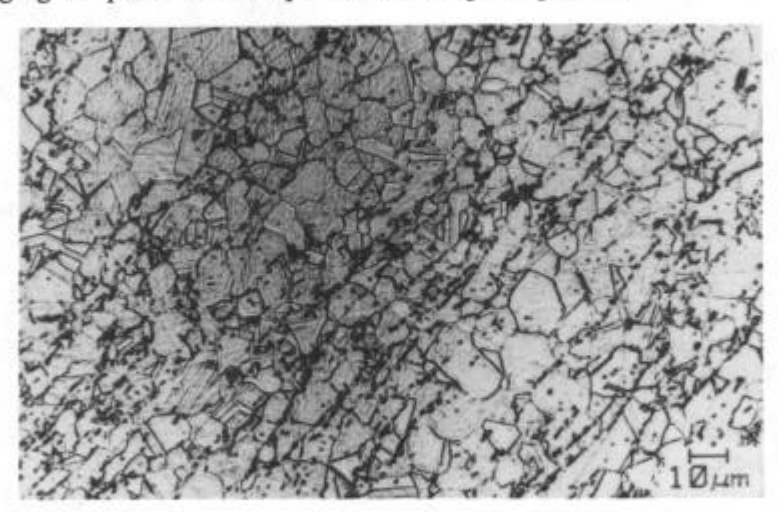


Figure 1 - Fine grain structure of directly aged alloy 718.

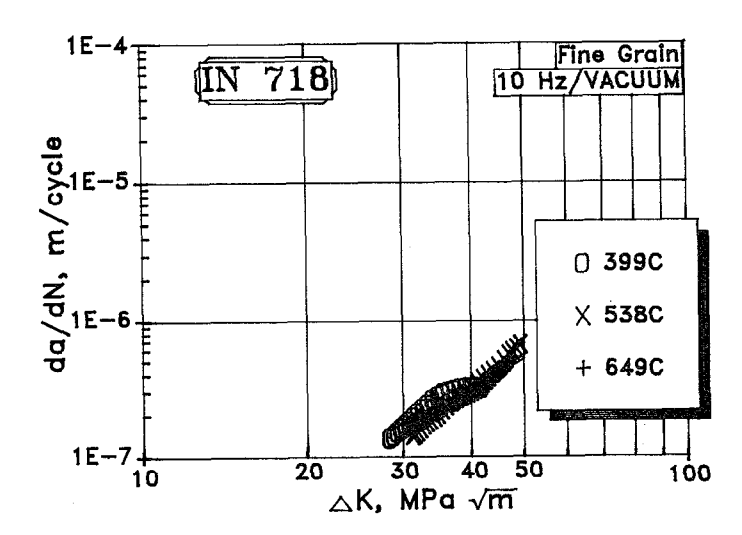


Figure 2 - Cycle dependent fatigue crack growth curves in alloy 718.

As proposed by Speidel [7], any differences in da/dN observed for materials operated under cycle-dependent conditions, e.g., room temperature in a vacuum environment, can be mainly explained by differences in elastic modulus. Normalizing  $\Delta K$  by the elastic modulus can unify fatigue crack growth rates measured for a wide variety of alloy systems. Testing parameters, such as cycle period and wave form, play a negligible role in determining how fast the crack will grow for a fixed  $\Delta K$ . In fact, the Stage II fatigue crack growth rate has been considered to be insensitive to the variations in microstructure and alloy chemistry [8].

Figure 2 compares the fatigue crack growth rates of alloy 718 measured in the cycle-dependent domains. The frequency of fatigue cycles was 10 Hz. These high temperature tests (399, 538, and 649 °C) were conducted in vacuum. Clearly the crack growth curves fall on one another within the experimental accuracy. The results agree with room temperature da/dN data. Such a universal crack growth rate can be considered as the rate simply contributed by the pure mechanical driving force as defined by linear elastic fracture mechanics (LEFM). It will be used as the baseline to evaluate the crack growth resistance under different testing conditions.

At low temperatures in air, the frequency and the waveform of fatigue cycles may not influence the crack growth rate. FCP data measured by two fatigue frequencies, 3 s/cycle and 180 s/cycle, tested at 399 °C, were in good agreement with those shown in Figure 2. The da/dN value is only a function of  $\Delta K$ , independent of the fatigue frequency.

However, a substantial increase in da/dN occurred at slow fatigue cycles when the temperature was raised to 593 °C (Figure 3). A factor of 5X was observed for a given  $\Delta K$  when the fatigue frequency changed. The 177-s sustained loading at the peak load of each fatigue cycle further degraded the crack growth resistance, and da/dN increased by 10X with respect to 3-s cycles.

Such a time-dependent FCP has been observed in many high-strength superalloys, and the mechanism can be explained by a damage zone model based on stress oxidation cracking [9]. Under an applied stress intensity, oxygen from the air environment interacts dynamically with the material in front of the crack tip. As a result, oxygen-embrittled material forms a damage zone ahead of the crack. The kinetics of embrittlement are

thermally activated, and the degree of damage is a function of the distance from the crack tip and the time for embrittlement. The crack can propagate at a much faster rate in the damage zone than in the undamaged material, under the same driving force,  $\Delta K$ .

Examining the fracture surface revealed the change of fracture mode as different fatigue frequencies or cycle waveforms was used. At the fast frequency, cracks propagated transgranularly with conventional fatigue striations as seen in Figure 4(a). When a slow frequency (180 s/cycle) or a hold-time waveform (3+177 s/cycle) was applied at elevated temperatures, the crack growth rate was accelerated substantially, and cracks fractured intergranularly. Grain boundary decohesion in a brittle manner is evident in Figure 4(b), which consists of many featureless facets of grain boundaries. This observation is in consistent with the time-dependent mechanism associated with the stress oxidation cracking.

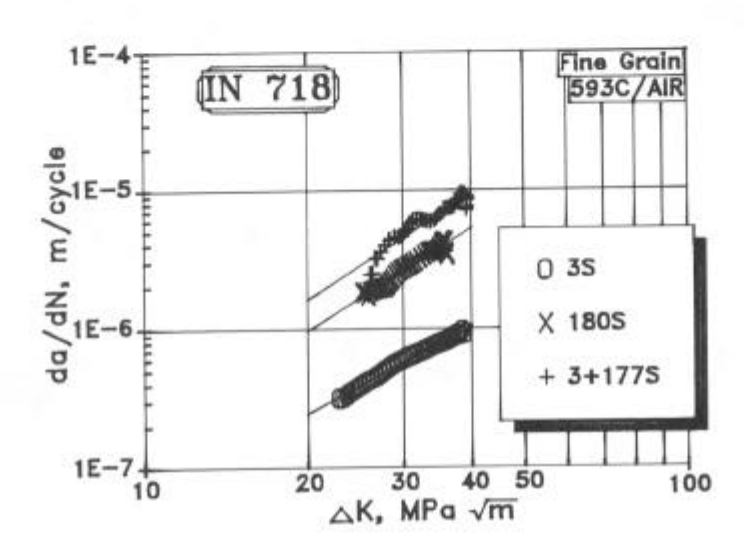


Figure 3 - Time-dependent fatigue crack growth curves (593 °C) in alloy 718.

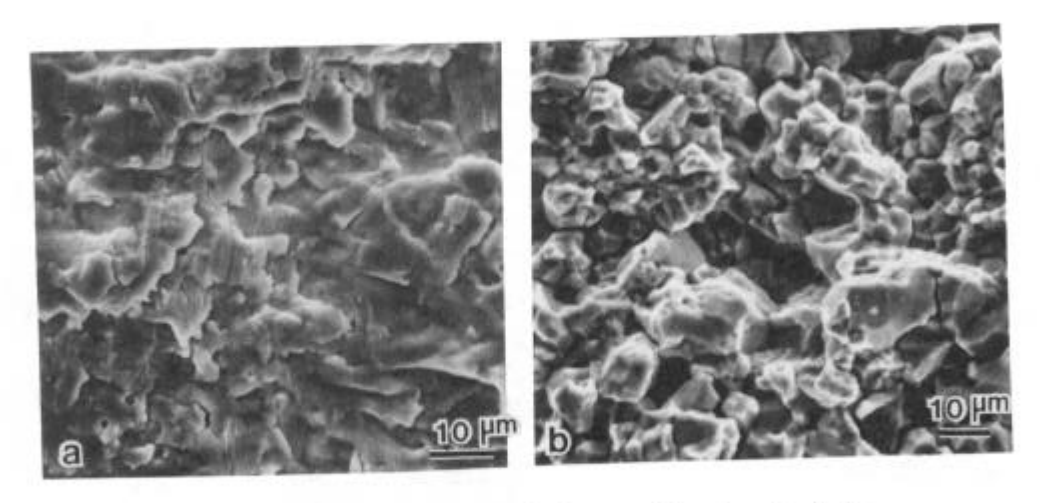


Figure 4 - Fracture modes of fatigue cracking in alloy 718: (a) cycle dependent; (b) time dependent.

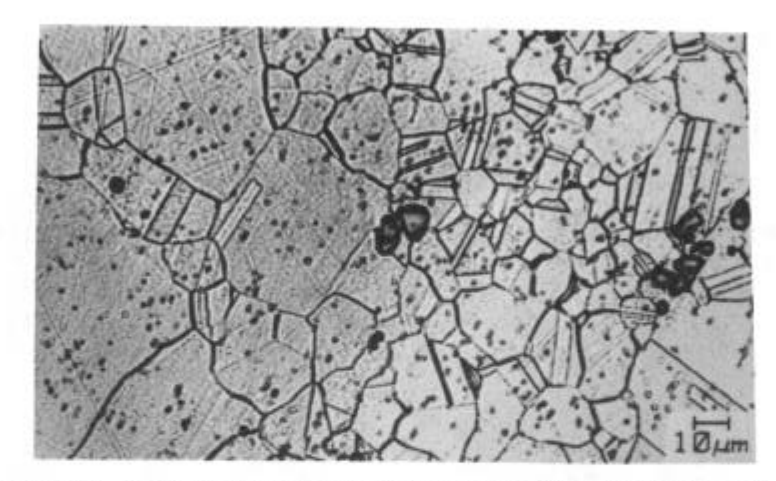


Figure 5 - Coarse grain structure of annealed (1025 °C) alloy 718.

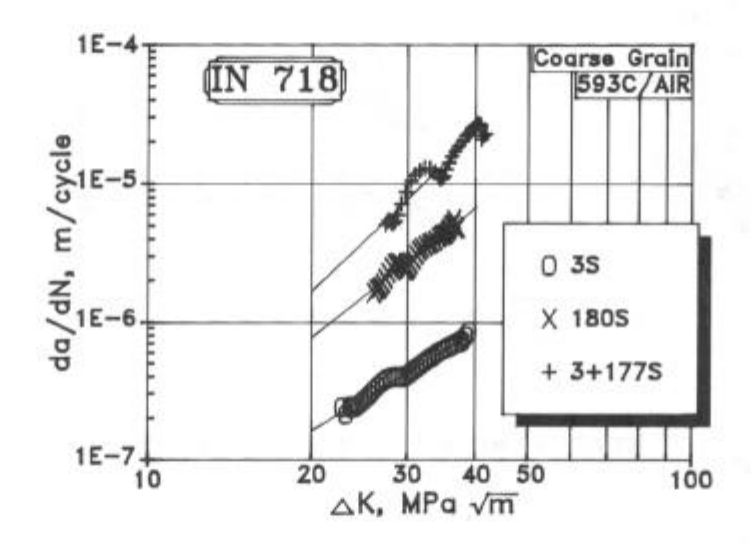


Figure 6 - Fatigue crack growth curves (593 °C) in coarse-grain alloy 718.

Table 1. Crack growth rates (m/cycle) measured at 593 °C in vacuum for coarsegain and fine-grain alloy 718.

		$\Delta K$ ,		
Grain Size	Waveform	23	28	33
Fine Grains	3 s	7.04E-8	1.03E-7	1.95E-7
	180 s	7.68E-8	1.23E-7	1.77E-7
	3+177 s	5.65E-8	1.00E-7	1.49E-7
Coarse Grains	3 s	7.12E-8	1.48E-7	2.36E-7
	180 s	7.33E-8	1.43E-7	1.89E-7
	3+177 s	6.03E-8	1.06E-7	1.91E-7

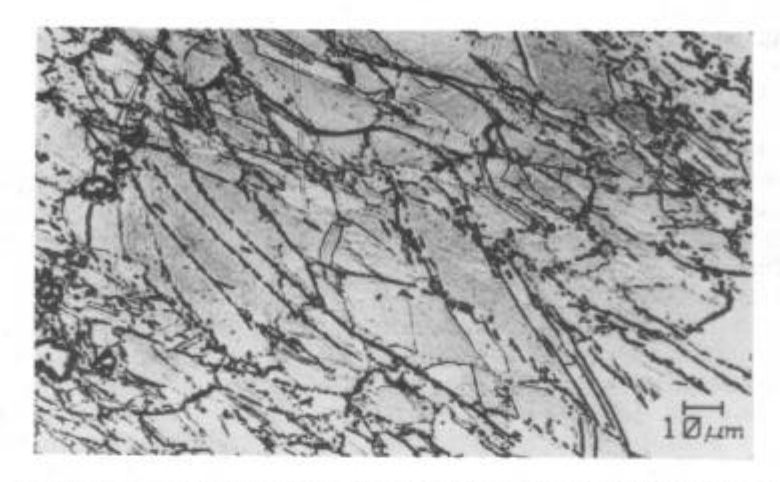


Figure 7 - Deformed grain structure of alloy 718 observed at a forging surface.

## Grain Size Effect

The fine grain structure observed in the as-received forging was attained by the existence of uniformly distributed  $\delta$ -Ni<sub>3</sub>Nb precipitates. An annealing treatment at a temperature above their solvus, e.g., 1025 °C, can dissolve these precipitates and grow the grain size. Figure 5 shows the grain structure after one hour solution anneal at 1025 °C. Equiaxed grains of ASTM 7 (35  $\mu$ m) were developed; the microstructure looks equiaxed. Compared to Figure 1, the 1025 °C anneal removed all stringered precipitates, and only isolated carbides remained.

After aging treatments, the solution-annealed alloy 718 was tested at 593 °C by three fatigue cycles as described previously. The results are plotted in Figure 6. In spite of a significant difference in grain size, coarse-grain and fine-grain structures had a similar crack growth behavior. A strong time dependence of da/dN was observed in the annealed alloy 718, and the major fracture mode changed from transgranular striations to grain boundary splitting.

Under the fast fatigue frequency (3 s/cycle), alloy 718 with a coarse-grain structure seemed to have a crack growth rate somewhat lower (30%) than that with a fine-grain structure. Though the da/dN value did not match exactly that in Figure 2, this grain size effect was considered to be valid in the cycle dependent domain. The fracture mode was transgranular, and the grain size is believed to modify the mechanical driving force for cracking. A similar grain size effect has been reported in alloy 718 tested at 427 °C [10].

Coarse grains did not help the fatigue cracking resistance in the time-dependent domain. A slightly higher da/dN was measured in the annealed ally 718 under the hold-time waveform (3+177 s/cycle). However, the crack growth rate returned to the cycle-dependent value if tested in vacuum. Table 1 lists some da/dN data measured from both coarse-grain and fine-grain structure at selected  $\Delta K$  values. No difference in the crack growth rate was found among different fatigue waveforms for a given  $\Delta K$ . Without an oxidation environment, the cracking is simply determined by the mechanical driving force, and the fracture remains intergranular.

## Deformed Grain Structure

When the specimens were cut from different locations through thickness of the asreceived disk forging, different grain structures were observed. At locations near the surface, a deformed grain structure indicated the lack of recrystallization during the forging operation (Figure 7). The chilling effect associated with the contact of dies during forging prevented this region from the dynamic recrystallization that occurred in the center portion of the disk. Subsequent heat-treatments only involved aging steps without a high temperature anneal to allow any recrystallization reaction. As a result, the surface region consists of coarse elongated grains. The average grain size was ASTM 6. Precipitate stringers were aligned along flow lines. The SEN specimen was oriented in a direction such that the crack propagated normal to the flow lines of forging. The FCP data measured at 593 °C are shown in Figure 8. The deformed grain structure exhibited very little time dependence in crack growth rate when the fatigue frequency was changed. The hold-time waveform (3+177 s/cycle) even slowed da/dN down below that measured by the fast frequency cycles (3 s/cycle).

A series of laboratory heats with the nominal alloy 718 composition was prepared to confirm the effect of deformed grain structure. Two forged plates were heated to 1075 and 1025 °C, respectively. The forging condition was simulated by the rolling of 50 % reduction in thickness through four passes. The mass of the forging plates was so small that a substantial temperature drop occurred during rolling. Metallography showed an elongated grain structure similar to that seen in Figure 7. Because the rolling finish temperature was much lower than the recrystallization temperature (950 °C), the deformed grains did not contain any fine recrystallized grain. These plates were subjected to aging treatments directly without solution annealing. Because of a significant amount of residual strains introduced by rolling, the alloys show improved strength over those being solution-annealed. The good resistance to fatigue cracking under time-dependent conditions was reconfirmed in the deformed grain structure. The results of yield strengths and crack growth rates are compared in Table 2 for different processing and heat-treatment schedules.

Further demonstrations of this effect associated with the deformed grain structure were performed by cold rolling. Forged plates of a coarse grain structure were rolled at room temperature with 20% and 40% reductions, respectively. Direct aging was applied after cold rolling. As shown in Table 2, a good fatigue cracking resistance was developed.

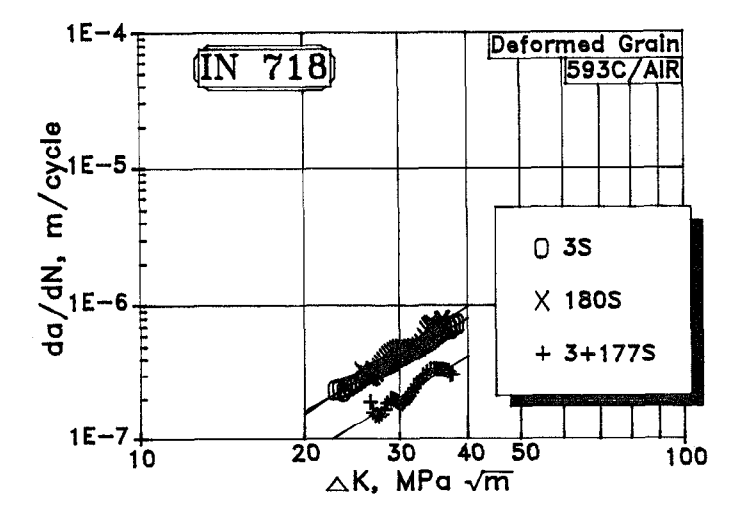


Figure 8 - Fatigue crack growth curves (593 °C) in deformed-grain alloy 718.

Table 2. Crack growth rates ( $\Delta K = 25 \text{ Mpa/m/593 °C}$ ) and yield strength (649 °C) of differently processed alloy 718.

	Strength	da/dN, m/cycle		
Processing	MPa	3 s	180 s	3+177 s
Annealed at 975 °C	978	2.57E-7	1.61E-6	4.87E-6
Rolled from 1075 °C Rolled from 1025 °C	1169 1218	1.81E-7 1.84E-7	2.87E-7 2.66E-7	3.41E-7 6.41E-8
Cold-rolled 20% Cold-rolled 40%	1295 1336	2.07E-7 2.27E-7	4.40E-7 2.00E-7	9.44E-8 8.01E-8

# **Chromium Addition**

Many superalloys develop their oxidation resistance by the addition of a large amount of Cr. Since the time dependent FCP is caused by stress oxidation cracking, we expect that the Cr content could play an important role for fatigue cracking resistance.

A series of laboratory heats was designed to have 12, 18, and 24 (in wt.%) of Cr contents in alloy 718. An equal amount of Fe was substituted for Cr to maintain the alloy strength. The forgings received the standard heat treatments including the solution annealing and the double aging. These alloys exhibited a similar grain structure, and their yield strengths were almost the same. The crack growth rate was measured at 538 °C by three fatigue waveforms used above. Figure 9 compares measured da/dNs as a function of the Cr content. At fast frequency (3 s/cycle), the three alloys had similar crack growth rates. The chromium effect appears under slow fatigue cycles or hold-time waveforms. At a low Cr content (12%), an order of magnitude increase in da/dN was found by slowing down the fatigue frequency. In contrast, the high Cr (24%) heat exhibited almost identical crack growth rates for all three waveforms.

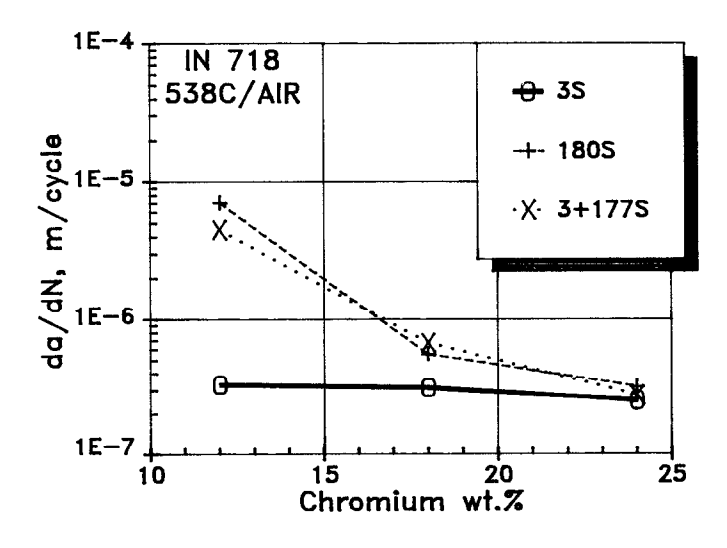


Figure 9 - The Cr effect on da/dN in alloy 718 ( $\Delta K = 30 \text{ Mpa/m/593 °C}$ ).

The fracture mode observed on the fracture surfaces can be correlated to the crack growth systematically. The 24Cr heat showed transgranular striations in all cases; no time dependent FCP was detected. As soon as the da/dN started to accelerate in the 18Cr heat, some intergranular fracture became evident. Complete grain boundary failure occurred in the 12Cr heat under the slow frequency or the hold-time cycles.

#### Conclusion

Alloy 718 shows the same fatigue cracking behavior as other high-strength supealloys. Two crack propagation domains, cycle dependent and time dependent, are identified. Stress oxidation cracking is the mechanism causing the acceleration of crack growth rate in the time dependent domain.

Two metallurgical factors have been found to improve the fatigue cracking resistance under the time dependent condition:

- 1. a deformed grain structure, and
- 2. Cr additions.

In the cycle dependent domain, the crack growth rate is dominated by the cyclic stress intensity. Grain size variations have a minor effect on the crack growth rate.

## Acknowledgments

The author wishes to thank his colleague, Dr. M.F. Henry, for helpful critics on the manuscript.

#### Reference

- D.R. Muzyka and G.N. Maniar, in <u>Metallography</u>, ed. H. Abrams and G.N. Maniar, (Philadelphia, PA: ASTM, STP 557, 1974), pp. 198-219.
  J.F. Barker, D.D. Krueger, and D.R. Chang, in <u>Advanced High-Temperature Alloys</u>,
- 2. J.F. Barker, D.D. Krueger, and D.R. Chang, in <u>Advanced High-Temperature Alloys</u>, ed. S. Allen, R. M. Pelloux, and R. Widmer., (Metals Park, OH: ASM, 1986), pp. 125-137.
- 3. R.A. Sprague and S.J. Friesen, J. Metals, 38 (1986), 24-30.
- 4. K.-M. Chang, Time-Dependent Mechanisms of fatigue Crack Propagation in High-Strength Superalloys, (GE-CRD Report 89CRD116, June 1989).
- 5. J.F. Radavich and W.H. Couts, Jr., in Superalloys 1984, ed. M. Gell et al., (Warrendale, PA: TMS, 1984), pp. 497-507.
- 6. K.-M. Chang, in <u>Effects of Load and Thermal Histories on Mechanical Behavior of materials</u>, ed. P.K. Liaw et al., (Warrendale, PA: TMS, 1987), pp. 13-26.
- 7. M.O. Speidel, in <u>High Temperature Materials in Gas Turbines</u>, ed. P.R. Sahm and M.O. Speidel, (New York, NY: American Elsevier Publishing Company, 1974), pp. 207-251.
- 8. M.E. Fine and R.O. Ritchie, in <u>Fatigue and Microstructure</u>, ed. M. Meshii, (Metals Park, OH: ASM, 1979), pp. 245-278.1
- 9. K.-M. Chang, M.F. Henry, and M.G. Benz: JOM, 18 (Dec. 1990), pp. 29-35.
- D.D. Krueger, S.D. Antolovich, and R.H. Van Stone, Met. Trans. A, 18A (1978), pp. 1431-1449.